ARTICLE IN PRESS

Available online at www.sciencedirect.com
ScienceDirect
Journal of Nuclear Materials xxx (2007) xxx–xxx
journal of nuclear materials
www.elsevier.com/locate/jnucmat

Volatile fission product behaviour during thermal annealing of irradiated UO_2 fuel oxidised up to U_3O_8

J.-P. Hiernaut *, T. Wiss, D. Papaioannou, R.J.M. Konings, V.V. Rondinella

European Commission, Joint Research Centre, Institute for Transuranium Elements, P.O. Box 2340, 76125 Karlsruhe, Germany

Received 4 October 2006; accepted 15 March 2007

Abstract

The behaviour and release of fission products during high-temperature annealing of irradiated UO_2 samples have been studied as a function of the oxidation state. The behaviour of a sample pre-oxidised to U_3O_8 was compared to that of non-pre-treated fuel from the same pellet radial location. The Knudsen cell mass spectrometer technique was used up to 1900 K for the pre-oxidised sample and up to 2800 K for the untreated sample. Both types of tests were run in vacuum. The possible chemical forms of the different fission products in the bulk and in the vapour phase have been estimated from the release curves and microprobe analysis. This study concerns essentially iodine, tellurium, caesium, rubidium, strontium, barium, technetium and molybdenum, whose effusion behaviour was strongly affected by the pre-oxidation treatment, resulting in an almost complete release by 1900 K. Release of zirconium, the lanthanides and actinides was observed at temperatures >1900 K, reached only in the case of the non-pre-treated UO_2 experiments.

1. Introduction

The distribution and behaviour of fission products formed in nuclear fuel during in-pile operation are of importance to assess the operational performance and safety of the fuel, the possible consequences of severe accidents, and also the long-term corrosion behaviour of spent fuel after final disposal in a repository.

The behaviour of fission products in uranium oxide fuel is initially governed by their chemical state and by their mobility in the UO_2 bulk. Their eventual release depends also on additional mechanisms: e.g. trapping in bubbles for fission gases, or creation of intermediate phases for chemically reactive fission products (Cs, Rb, I, Te, Ba, Sr) [1,2]. During postulated severe reactor accidents, characterised by temperatures that significantly exceed the normal operation temperature and by ingress of air and steam, the release behaviour and the vaporisation rate of the fission products from the nuclear fuel depend drastically on the surrounding atmosphere, mainly on the concentration of oxygen defining the oxygen potential [3–5].

The non-volatile fission products may be classified in two categories: elements that are soluble in UO_2 or $(U,Pu)O_2$ (for example the lanthanides) and elements that are slightly soluble to insoluble (Mo, Ru, Pd, Rh, Tc). The vaporisation of the first

* Corresponding author. Tel.: +49 7247 951 385; fax: +49 7247 951 99 385.
E-mail address: Jean-Pol.Hiernaut@ec.europa.eu (J.-P. Hiernaut).

0022-3115/$ - see front matter © 2007 Elsevier B.V. All rights reserved.
doi:10.1016/j.jnucmat.2007.03.174

group is detectable above 2000 K together with the vaporisation of the fuel matrix, the measured vaporisation enthalpies ranging between 501 and 548 kJ mol^{-1}, close to the enthalpy of vaporisation of Ln_2O_3 [6]; the measured vapour pressures above irradiated fuel show an activity equal to their concentration in the fuel [7,8]. Atoms of the second group (Mo, Pd, Rh, Ru, Tc) precipitate in form of metallic particles mainly located in voids, bubbles, or at the grain boundary [9–11]. These metals have a low vapour pressure and are generally not released at low temperature from hypo to stoichiometric fuel. Some of these species (e.g. Mo) can also be present as components of perovskite-like ABO_3 compounds (where A = Sr, Ba, B = U, Pu, Zr, Mo) segregated at grain boundaries, the so-called grey phase [5].

In hyperstoichiometric uranium oxide, the release of volatile fission products will be enhanced by favourable changes of the diffusion coefficient, and by the structural transformation of the fuel. Additionally, the very high volatility of the matrix itself will boost the release of volatile fission products [12]. Furthermore, due to the high oxygen potential, redox-sensitive non-volatile fission products like Mo and Tc will change their valency, be oxidised into volatile oxides (MoO_3, TcO_2) and released.

If the fuel is oxidised to compositions close to U_3O_8 the high oxygen potential permits to oxidise elements that are normally in the metallic state, e.g. Mo, Tc or Te, and eventually makes the formation of complex phases more likely, e.g. (Ba,Sr)-MoO_4, Cs_2MoO_4, Cs_2TeO_4, Cs_2UO_4, (Ba,Sr)UO_3 or (Ba,Sr)UO_4 [13,14]. Most of these oxides and compounds have been studied by Knudsen cell mass spectrometry [13,15–19], or postulated from redeposition studies in simulated accident conditions [20–22]. In the latter experiments the O/U of the fuel and the release of fission products are governed by the reaction water vapour-cladding-fuel [23,24].

Most of the information available from the literature comes from experiments performed on analogues, or on specific constituents of the fuel system. This type of investigation allows a detailed thermodynamic characterisation of phases considered relevant for the behaviour of irradiated fuel. However, it misses the effects due to the complex set of interactions occurring among the multitude of species present in the real irradiated fuel. Although not so unequivocal in the interpretation of the results, the integral study of the release of fission products and actinides from irradiated fuels under laboratory annealing conditions permits to observe directly the behaviour of the fuel at high-temperature, to obtain representative data suitable for the mechanistic analysis of the mass migration process in the fuel, especially at high burn-up, and for the determination of the risk associated with severe in-pile temperature transients or reactor disruptive accidents. Additionally, the vaporisation measurements for the species contained in the matrix permit to validate the thermodynamic models for irradiated fuel containing fission products, to predict the chemical reactions occurring during reactor accidents, and thus to predict the chemical state of the radio-toxic nuclides released.

In the present study we have used a high-temperature Knudsen cell combined with a mass spectrometer that can measure the release of fission products and the matrix vaporisation behaviour on irradiated fuel samples up to 3000 K. The measurements have been carried out on samples oxidised before the experiment to the U_3O_8 level. The results have been compared to the release behaviour from a sample of the same UO_2 fuel not subjected to pre-oxidation treatments. These experiments permitted studying the effect of high oxygen potential conditions, typical of reactor disruptive accidents, on the fission products release.

2. Experimental and samples

The experimental set-up combining a Knudsen cell with a quadrupole mass spectrometer was described earlier [1,4]. All the annealing experiments were performed in vacuum. A heating rate of 30 K/min was used in all experiments. A total of three fuel samples were analysed: two samples oxidised to U_3O_8 in air at 670 K [1] prior to the Knudsen cell experiment, and one 'as-stored', i.e. with the O/U developed during irradiation and the subsequent standard post-discharge life (cooling pool, hot cell). The annealing experiments on oxidised fuel were performed in the temperature range 300–1950 K using alumina crucibles. The 'as-stored' specimen was analysed between 300 K and 2800 K in a tungsten cell [4].

The samples were described in detail in [3]. They were small pieces (10–20 mg) of BWR UO_2 with 65 GWd/t taken from a region close to the cladding. The morphology of the samples was examined before and after annealing by scanning electron microscopy (Philips XL40) equipped with an energy dispersive X-ray analysis system (EDX), which provided information on phase composition. The crystallographic structure of the oxidised fuel

Please cite this article in press as: J.-P. Hiernaut et al., J. Nucl. Mater. (2007), doi:10.1016/j.jnucmat.2007.03.174

matrix was studied in a previous paper [4]. The metallic precipitates were analysed by EDX using a standard-less method. EDX analysis on several metallic particles of the non-oxidised fuel was in good agreement with their nominal composition [7]. A statistical analysis of the results is given in Section 4.3.

All masses between 83 and 300 were measured during annealing of the samples: fission products from Kr to Gd and actinides, in elemental, oxidised or in more complex form. The ionisation electron energy was 40 eV, sufficient to ionise all the species released including the noble gases (He, Kr, Xe), but too high to avoid dissociation of complex molecules present in the vapour. No significant peaks were observed in the range 300–500 a.m.u. In this configuration it is not always possible to assign the signals of simple atomic species to the parent molecules in the vapour.

Certain peaks of the mass spectrometer spectrum were subject to interferences, i.e. MoO_2 with I and Te; MoO_3 with lanthanides. The ambiguity was generally solved by verifying the isotopic abundance of the elements or species. Moreover, in some cases the release of some elements did not occur as expected, in terms of the annealing temperature range (lanthanides) or of discrepancies between different species supposing origin from the same phase (TeO, MoO_3).

3. Analysis of the fission product release

The measured fractional release curves for the different fission products contained in the fuel were modelled using the fitting model EFFUS by Ronchi et al. [1,4,25], which describes the transport and release processes by a system of reaction rate equations expressing venting (vaporisation), diffusion (vaporisation), and trapping (phase formation–precipitation). Fig. 1 schematically illustrates the main conceptual steps of the model, which considers mainly gases to be present at grain boundaries, in solution, or precipitated in bubbles [4,25,26].

4. Results

The release of the noble gases He, Kr and Xe was analysed already in [4], where the release of some fission products was addressed as well. This paper focuses in detail on the chemical aspects of the release from highly hyperstoichiometric UO_2 fuel (U_3O_8), compared to a non-oxidised sample under 'as-stored' conditions. Furthermore, it aims at comparing the outcome of integral experiments that measure the release of multiple species from real irradiated fuel samples with single-phase data and hypotheses presented in the literature.

4.1. Irradiated UO_2 pre-oxidised to U_3O_8

Fig. 2 illustrates the effects of annealing in vacuum on the pre-oxidised fuel samples. Fig. 2(a) shows the change of the oxidation level of the fuel matrix (uranium dioxide) as a function of the absolute temperature during annealing in the Knudsen cell. The O/U ratio is calculated from the uranium signals using the ionisation and dissociation potentials as described in a previous paper [25]. The samples remained hyperstoichiometric up to

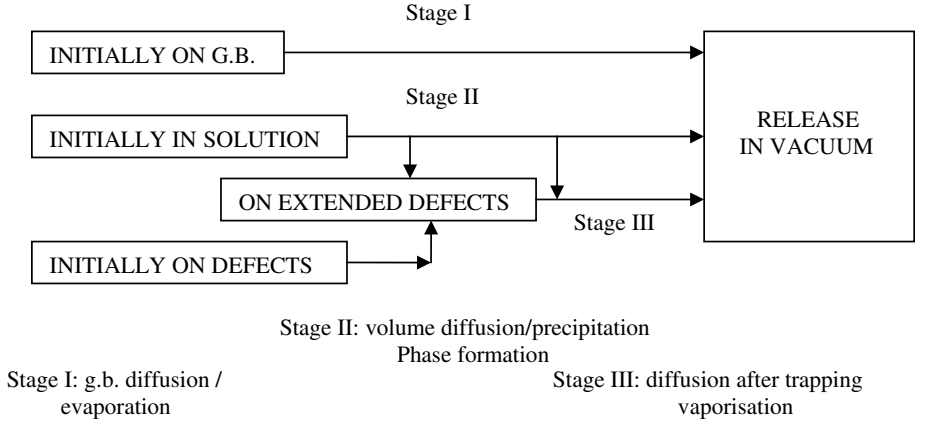

Fig. 1. Schematic representation of the fitting program EFFUS: 3 stages are considered, the first stage considers the fission products on the grain boundary, the other 2 stages consider the transport of fission product in solution to the surface and to defects precipitated in the bulk, or the release of species in extended defects via diffusion and/or matrix vaporisation.

Please cite this article in press as: J.-P. Hiernaut et al., J. Nucl. Mater. (2007), doi:10.1016/j.jnucmat.2007.03.174

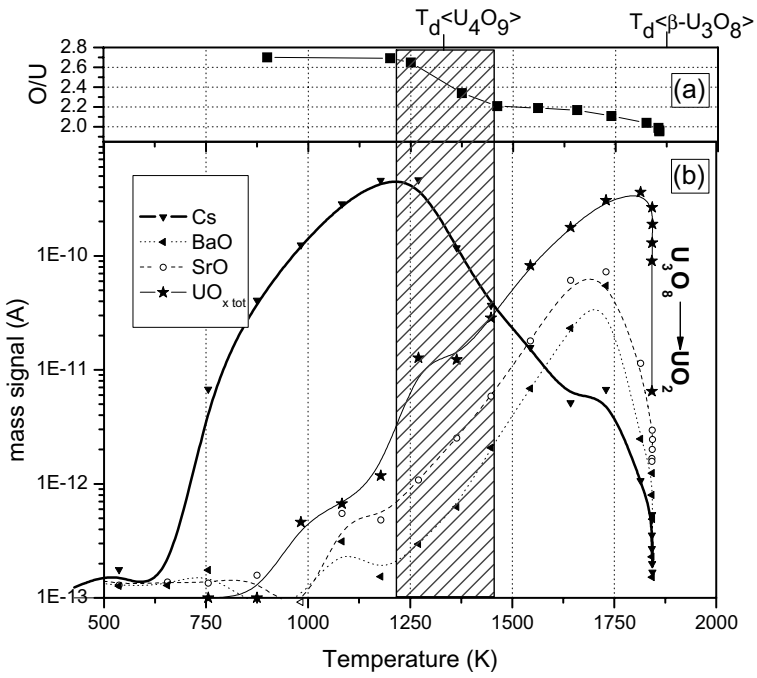

Fig. 2. (a) Change of the oxidation level of a pre-oxidised irradiated UO_2 sample, O/U, as a function of absolute temperature during the annealing in the Knudsen cell in vacuum calculated as described in [25]. (b) Corresponding mass spectrometry signals: release curves for uranium (sum of all species), Cs, BaO, SrO vs. temperature.

1850 K. No significant changes of O/U occurred up to 1250 K. The O/U of the samples reduced from the initial level to approximately 2.2 within a relatively narrow temperature interval between 1250 and 1450 K (shaded band in the figure). This O/U level remained stable up to 1600 K. Above this temperature the reduction accelerated again. O/U = 2.0 was reached at 1850 K. The corresponding release (see Fig. 2(b)) was marked by a drastic decrease of the signals for the uranium oxides around 1850 K. Fig. 2(b) reports the release curves as a function of the temperature for the uranium oxides (sum of mass spectrometry signals for UO, UO_2 and UO_3) and for Cs, BaO, SrO. Cs release started at relatively low temperature and reached its maximum intensity at 1250 K where the first reduction step of the O/U of the sample took place. BaO and SrO showed similar release behaviour trends, with the maximum level of mass spectrometer signal reached at approximately 1750 K, possibly in correspondence with the second reduction step for the sample. After 10 min at 1850 K in vacuum no mass spectrometry signals were further detectable for any U-oxide species, indicating that the sample was reduced. The same drop of the signal was observed for Cs, BaO and SrO, and for essentially all the other volatile fission products. However, visual inspection of the sample after the experiment revealed that only a minor fraction of the total mass of the sample had vaporised.

The fission products Cs, Mo, Te, I, Tc, Sr and Ba, were detected respectively in the form of Cs^+, CsI^+, Mo^+, MoO^+, MoO_2^+, MoO_3^+, Te^+, TeO^+, I^+, Tc^+, TcO^+, SrO^+, Ba^+ and BaO^+. Since the ionisation electron energy was kept constant at 40 eV, the electron energy was sufficient to ionise all the fission products, but also high enough to dissociate most of the complex molecules such as CsO_x, CsTe, or Cs_2MoO_4.

It is important to quantify the fraction of volatile fission products released during annealing of the oxidised fuel in the temperature range 300–1900 K, and to compare this fraction to the corresponding amount released from the 'as-stored' UO_2 sample in the same temperature interval. Table 1 summarises these quantities for all fission product species considered except Mo and Tc which were not observed in the case of non-oxidised fuel experiments because of their low vapour pressure in the temperature range considered (see Section 4.3). The released fraction of Mo and Tc from the pre-oxidised sample was estimated to be 80% and

Table 1
Fraction of fission products released in the temperature range 300–1900 K from UO_2 fuel oxidised (column 2) and non-oxidised (column 3)

Species	Fraction released up to 1900 K (%)	
	Oxidised samples	Non-oxidised sample
^{138}Ba	10	2
^{138}BaO	18	2
^{88}Sr	0	0.05
^{88}SrO	100	0
^{90}Sr	0	0.05
^{90}SrO	100	0
^{133}Cs	100	30
^{135}Cs	100	30
^{137}Cs	100	30
^{99}Tc	40	
$\sum Mo$	80	
^{87}Rb	100	30
^{127}I	100	20
^{129}I	100	20
^{128}Te	100	6
^{128}TeO	100	0
^{130}Te	100	6
^{130}TeO	100	0
$\sum UO_x(*)$	~10	~0

The fractions are normalised to the total inventory released in the experiment with non-oxidised fuel up to 2700 K, which completely vaporised the sample. Signal integrals normalised to sample weight are used to calculate the ratios.

40%, respectively, mainly due to oxide species. Columns 2 and 3 of Table 1 report the amount released in the range 300–1900 K from the oxidised and the 'as-stored' samples, respectively. The fractions are normalised to the amount measured during total evaporation of the non-oxidised sample in the extended range 300–2700 K. This experiment produced the complete vaporisation of the sample, hence the release of its total inventory. The data in the table show that the entire inventory of volatile fission products Cs, Rb, I, Te was released at $T \leqslant 1900$ K; Sr was entirely released as SrO while Ba, BaO were only partly released. The ratios reported in Table 1 also highlight that no substantial release occurred during the pre-oxidation treatment of the samples at 670 K (before the Knudsen cell annealing).

The fraction of UO_x that vaporised from the oxidised sample has also been evaluated from the mass spectrometry signals and normalised to the sample weight. During annealing of the oxidised samples approximately 10% of the fuel matrix vaporised; the release started around 1000 K and peaked at 1800 K in correspondence to its final reduction stage. In the same temperature range very low vaporisation occurred from the matrix of the non pre-oxidised sample; the first indications for UO_2 release became evident for $T \geqslant 1800$ K.

The release rate from the oxidised samples for the main isotopes of Cs, I, Rb, CsI, MoO_3, MoO, BaO, SrO, Te, TeO, Tc, TcO, TcO_3 is plotted as a function of. temperature in Fig. 3. The results for the two samples annealed were almost perfectly reproducible. The only detected discrepancy concerned the relative strength of the signals for different oxide species of Mo: for one sample MoO_3 was the main species, as expected because of its higher vapour pressure, while in the other case it was MoO.

MoO_2 is not shown in Fig. 3: it is difficult to evaluate this species accurately, since the signal interferes with I, Te and Xe. The assignment of a signal to an isotope of a given element (or compound) is based on the isotopic fingerprint of this element and on the parallelism of the signals of other isotopes of the same element. For clarity, only one isotope of each fission product is shown in Fig. 3; it has to be intended that the curves for all isotopes of a given element were always parallel, except when interferences with another element were present. In this case a decomposition of the signals was attempted, taking into account the isotopic composition as calculated with the ORIGEN-2 code.

Some species showed significant release distributed over a broad temperature range, starting around 750 K. The signals of almost all species reached a maximum: a first group peaked around 1250 K; a second group, characterised by a release concentrated in the high-temperature range (1100–1750 K), peaked at 1700 K. The signal for all species fell below the detection limit above 1850 K, like the uranium oxide species plotted in Fig. 2(b).

The release of iodine (^{127}I and ^{129}I) as shown in Fig. 3(top) begins at 600 K, shows two maxima in the release rate at 750 K and 1300 K and is complete at 1850 K. The first maximum is probably due to vaporisation of elemental iodine, the second due to the vaporisation of caesium iodide as it coincides with a small fraction of the $^{133}Cs^{129}I^+$ ion, about 1% of the total iodine signal (CsI is probably also dissociated by electron impact), measured at temperatures between 1000 and 1500 K, with the maximum release rate also near 1300 K. The formation of CsI in nuclear fuel has been predicted by thermodynamic calculations indicating that it is stable up to an oxygen potential >-200 kJ/mol O_2, above which it is unstable with respect to Cs_2MoO_4 and I_2 [26,27].

Please cite this article in press as: J.-P. Hiernaut et al., J. Nucl. Mater. (2007), doi:10.1016/j.jnucmat.2007.03.174

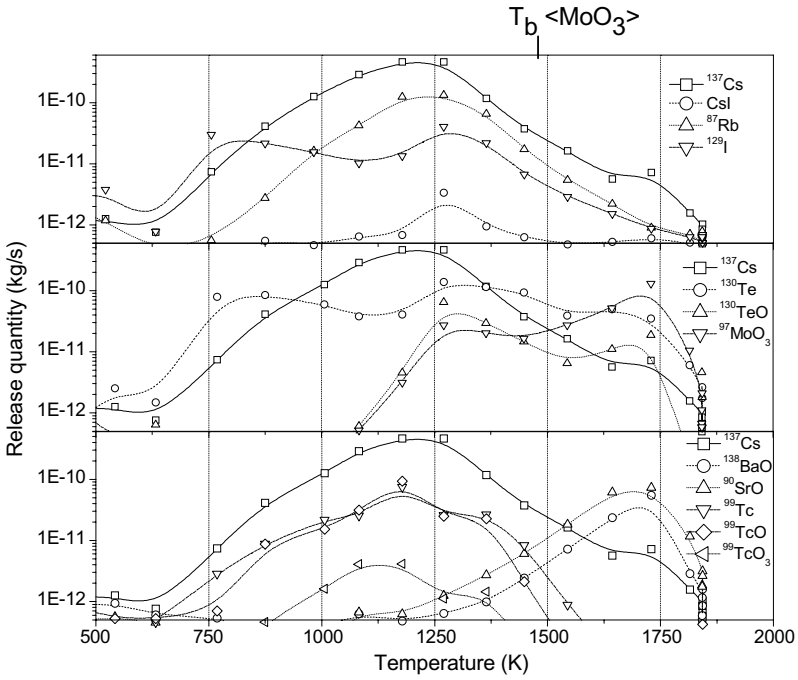

Fig. 3. Release rate of Cs, Rb, I, and CsI (top) Cs, TeO, Te (middle) and Cs, BaO, SrO, TcO, TcO_3 and MoO_3 (bottom) as a function of the absolute temperature from two pre-oxidised irradiated UO_2 samples.

The release curves of Cs and Rb (Fig. 3(top)) are almost parallel, release beginning at 600 K for Cs and at 800 K for Rb, reaching a maximum rate at about 1250 K, and indicating complete release at 1850 K. The signals of Cs and MoO_3 (Fig. 3(middle)) do not seem to be correlated, but this does not totally exclude the formation of Cs_2MoO_4. This compound, which vaporises congruently, but is likely fragmented by the ionising electrons of the mass spectrometer, is predicted to be the most stable caesium phase at high oxygen potentials [13,27,28]. In addition to CsI mentioned above, other possible caesium phases to be considered are Cs_2ZrO_3 and caesium uranates ($Cs_2UO_{3.5}$, Cs_2UO_4, $Cs_2U_4O_{12}$) [26,27], which decompose to give gaseous Cs or CsO species.

Tellurium is present in the fuel as oxide dissolved in the matrix, as oxide precipitate and as component of metal alloy precipitate [5]. It is likely that Te vaporises from different phases, since this species is released at non-negligible rates over the whole temperature range studied (Fig. 3(middle)). The release pattern of isotopes ^{128}Te and ^{130}Te is comparable to that of iodine between 600 and 1500 K. At $T > 1100$ K also TeO^+ is detected, with a release curve similar to Te^+ but about seven times smaller. It is likely that in the low temperature range Te originates from non-oxidised tellurium phases [26,27]. At low oxygen potential Cs_2Te could form in the fuel, which would vaporise incongruently to give principally Cs(g). At high oxygen potentials oxidation to TeO_2 or even Cs_2TeO_3 could occur, reducing the tellurium vapour pressure considerably.

In nuclear fuel molybdenum is a major component of metallic precipitates, which can contain Mo, Tc, Ru, Rh, Pd, the so-called 5-metal particles [5]. Mo is also present in precipitated oxide phases; it is assumed that Mo is transformed from one form to the other, buffering the oxygen potential of oxide fuels during in-pile irradiation [7]. The release curves of MoO and MoO_3 (Fig. 3(middle)) begin at 1100 K and show two maxima, one at about 1300 K, the other at 1700 K. These observations are consistent with the fact that the oxides of technetium and molybdenum are stable at lower oxygen potentials than those for the other constituents of the metal precipitates (see Fig. 7), and form volatile oxide species. Evidently the high oxygen potential leads to selective oxidation of these metals from the metal particles and subsequent vaporisation.

Of the other metals of these alloy precipitates, only technetium was also observed. Technetium (Fig. 3(bottom)) was found to be very volatile. It was detected mainly in one of the samples, in form

Please cite this article in press as: J.-P. Hiernaut et al., J. Nucl. Mater. (2007), doi:10.1016/j.jnucmat.2007.03.174

of Tc, TcO, and TcO_3 ionic species, the release maximum being at 1200 K. The release of all Tc species was complete at 1600 K, at a temperature level where the oxygen potential line of the system Tc/TcO_2 crosses the calculated oxygen potential curve of the Kc system during the annealing of the oxidised samples (Fig. 7). The maximum temperature is also close to the sublimation temperature of TcO_2, 1200 K [28]. The detection of TcO_3 in the vapour, a clear indication that the species arises from oxidised material, could indicate the presence of oxidised technetium in the sample, possibly oxide precipitate phases associated with Cs, Rb, Sr such as $CsTcO_4$, $RbTcO_4$, $Sr(TcO_4)_2$ [29].

Barium and strontium (Fig. 3(bottom)) are detected at $T \geqslant 1100$ K, as Ba^+ and BaO^+ and SrO^+ (no Sr^+ was detected). In nuclear fuel these elements, especially Sr, can dissolve in the UO_2 lattice, from which they can precipitate in the thermodynamically stable phase $(Ba,Sr)(Zr,U,Pu)O_3$, the so-called grey phase [7]. These are the most likely sources for BaO and SrO. The good correlation between the second MoO_3 maximum (well above its boiling point of 1430 K) and BaO, SrO and also with UO_3 (Figs. 2 and 3) suggests that these fission product species are released in the same process. The formation of $(Ba,Sr)MoO_4$, which vaporises congruently, could be proposed. Remarkably, Table 1 shows that the release of Sr (as monoxide) is complete at 1900 K, whereas only 10% of Ba and 18% of BaO are released at that temperature. This would suggest that $SrMoO_4$ is significantly more stable than $BaMoO_4$. This is confirmed by the fact that the Gibbs energy of the reaction

$$MZrO_3(cr) + MoO_3(cr) = MMoO_4(cr) + ZrO_2(cr)$$

is indeed about 100 kJ mol^{-1} more negative for M = Sr compared to M = Ba.

The behaviour of these fission product compounds was studied using the EFFUS model, developed mainly for gases [4]. The effusing species can be in solution in the bulk, or precipitated in complex chemical form and diffusing to the grain boundaries, or already located at grain boundaries, where they could react in presence of oxygen with other fission products to form different complex phases. The stability and/or the volatility of these phases are the determinant release steps. Three main stages are identified in this model as describing the release process. The results for the three stages determined by the fitting (with a precision generally better than 1.5%) of the normalised fractional release of the fission products considered (except Tc) are given in Table 2.

Stage I concerns the diffusion–vaporisation of phase compounds located at the grain boundary. Only Cs, Rb, I and Te are detectable in the temperature range 600–1000 K. The enthalpies of diffusion (or sublimation of low stability phases), determined with a relatively poor precision, are small, between 33 and 116 kJ mol^{-1} and could correspond to the vaporisation of I_2, CsI, CsTe, TeO_2. Simulations done in Knudsen cell by mixing CsI, Mo and $UO_{2(+x)}$ [13] result in sublimation enthalpies slightly higher (93–194 kJ mol^{-1}), but these values are highly dependent on the mixture and stoichiometry of all the reactants, so a direct comparison with the irradiated fuel system may not be fully representative.

The enthalpies of diffusion or vaporisation–sublimation for the main stages II and III were also independently obtained (van't Hoff law) from the linear range slope of $\ln(I_iT)$ vs. $1/T$ graphs in the related temperature ranges, where I_i is the mass spectrometric signal of the isotope or isotope compound 'i' and T the absolute temperature, and where (I_iT) is proportional to the vapour pressure p. The (release) enthalpies of Cs and Rb in stage II are about 95 kJ mol^{-1}, of the same order as the vaporisation enthalpy of metallic Cs (85 kJ mol^{-1}) and half the vaporisation enthalpies of caesium or rubidium oxides [6]. Iodine, Te, TeO, MoO_3, are released in a process having vaporisation enthalpies around 250 kJ mol^{-1}, higher than the corresponding value for TeO_2 [19]. Barium vaporises as Ba and BaO with vaporisation enthalpies, respectively, of 307 kJ mol^{-1}, and 277 kJ mol^{-1}, Sr vaporises exclusively as SrO with an enthalpy of 304 kJ mol^{-1}. They are close to the vaporisation enthalpy of U_3O_8 and MoO_3.

4.2. Comparison with non-oxidised irradiated UO_2

Fig. 4(a) illustrates the release behaviour of fission products from a sample of the same irradiated UO_2 pellet annealed in vacuum without prior oxidation treatment up to total vaporisation and Fig. 4(b) the evolution of its stoichiometry during thermal annealing. The main difference between these results and those described in the previous sections are:

- Cs, I, Te, Ba, Sr release occurs at temperatures 500–1000 °C higher than for oxidised fuel.

Table 2
Release steps, temperature of maxima, yields (in relative units), and process enthalpies (ΔH of diffusion at the grain boundary or in the bulk, of sublimation–vaporisation of element or compounds present in different phases or chemical forms) obtained from EFFUS calculations, (fit of the normalised fractional release) for the main volatile fission products, for a pre-oxidised sample

Fission product	T_{max} (K)	ΔH_I (kJ) Yield	T_{max} (K)	ΔH_{II} (kJ) Yield	T_{max} (K)	ΔH_{III} (kJ) Yield	Fit precision (%)
Cs	800	64.9 ± 4.3 *0.1*	1250	95.4 ± 0.83 *0.8*	1700	376.1 ± 3.3 *0.1*	0.3
Rb	800	$\sim 116.4 \pm 0.4$ *0.1*	1250	94.7 ± 1.1 *0.8*	1700	52.4 ± 2.6 *0.1*	0.4
I	800	33.3 ± 4.3 *0.4*	1300	241.3 ± 1.6 *0.4*	1700	9 ± 9 *0.2*	0.7
Te	800	43.9 ± 7.5 *0.3*	1300	247.9 ± 0.9 *0.4*	1700	68.9 ± 7.5 *0.3*	0.77
TeO	–	–	1300	252.9 ± 1.2 *0.65*	1700	406 ± 16 *0.35*	1.61
MoO_3	–		1300	127.4 ± 2.9 *0.3*	1750	368.9 ± 6.1 *0.7*	2.4
Ba	–	–	–	–	1750	307 ± 8 *1.0*	1.4
BaO	–	–	–	–	1750	277.1 ± 8.8 *1.0*	0.8
SrO	–	–	–	–	1750	303.7 ± 4.3 *1.0*	1.1
UO_3					–	342 ± 1	0.4

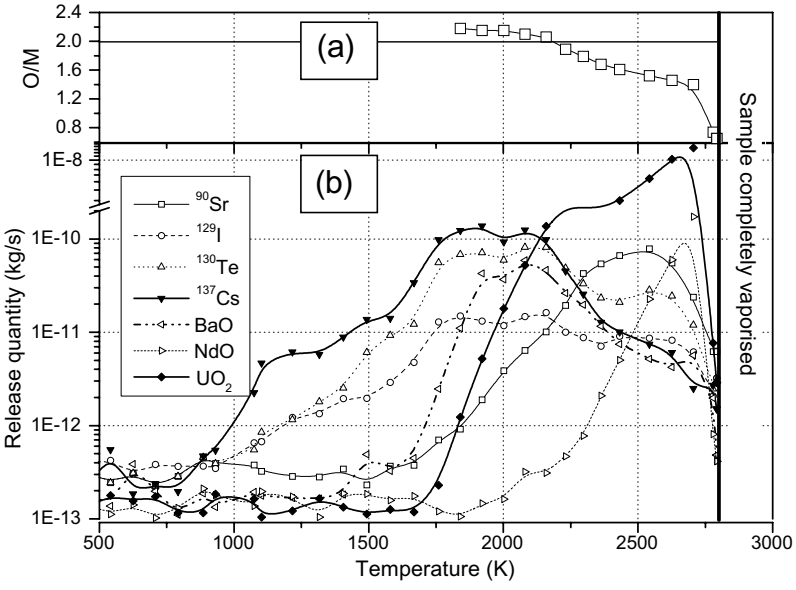

Fig. 4. (a) Change of the oxidation level of a non pre-oxidised irradiated UO_2 sample, O/U, as a function of absolute temperature during the annealing in the Knudsen cell in vacuum up to its total vaporisation [25]. (b) Corresponding mass spectrometry signals: release rate of Cs, I, Te, BaO, Sr, NdO as a function of the absolute temperature.

Please cite this article in press as: J.-P. Hiernaut et al., J. Nucl. Mater. (2007), doi:10.1016/j.jnucmat.2007.03.174

- Sr, releasing between 1700 and 2500 K, is only present as Sr^+, no more SrO^+, and Ba, between 1600 and 2100 K, only as BaO^+; the signal for Ba^+ corresponds to the electro-decomposition product of BaO.
- Tc^+, TcO^+, Mo^+, MoO^+, MoO_2^+ and MoO_3^+ are no longer detectable. The vapour pressure of metallic Mo and Tc are much too low in the temperature range up to 1900 K ($p = 10^{-7}$ and 10^{-6} Pa, respectively, at 1900 K).
- The main uranium species in the vapour at high-temperature is now UO_2^+, instead of UO_3^+, as expected and previously observed in the case of non pre-oxidised fuel annealed in vacuum ($O/U \leqslant 1.99$).
- The lanthanides are all detectable above 2200 K as Ln^+ and LnO^+. These species are all dissolved as oxides in the UO_2 matrix. The vapour pressures of the LnO_x species follow Henry's law meaning that their activities are close to their concentrations.

As in the previous experiments, the release of the different isotopes and compounds of every element are similar and the isotopic abundance are in agreement with the calculated inventory, and with the abundance measured in the previous sections for volatile fission products, except Ba. The results of the fit, using the EFFUS model, are summarised in Table 3.

No release was detected in stage I, while the maximum temperature of stage II is shifted up by 600 °C compared to the pre-oxidised sample. The enthalpies of diffusion–vaporisation are much higher than for the oxidised samples. Stage III is also shifted to higher temperatures by 400–600 °C; lanthanides have vaporisation enthalpies close to the literature values [6] for LnO and Ln_2O_3. Finally, the fuel vaporises with the enthalpy of sublimation of $UO_{1.99}$.

4.3. Microscopic observation and EDX study of the metallic precipitates

The metallic precipitates have been observed and analysed by SEM–EDX in the non-oxidised as well as the oxidised sample, both annealed at 1900 K. Fig. 5 illustrates some results of the SEM examination: the pictures in the figure are representative of the morphology of the two samples after annealing. Pictures (a) and (b) refer to the non-oxidised sample, while pictures (c) and (d) show the morphology

Table 3
Release steps, temperature of maxima, yields (in relative units), and process enthalpies (ΔH of diffusion at the grain boundary or in the bulk, of sublimation–vaporisation of element or compounds present in different phases or chemical forms) obtained from EFFUS calculations, (fit of the normalised fractional release) for the main volatile fission products, for a non-oxidised sample

Fission product	T_{max} (K)	ΔH_{II} (kJ) Yield	T_{max} (K)	ΔH_{III} (kJ) Yield	Fit precision %
Cs	1850	366.1 ± 1.7 *0.6*	2100	440 ± 0.3 *0.4*	1.2
Rb	1850	360.3 ± 2.1 *0.6*	2100	$\sim 416 \pm 0.4$ *0.4*	2.5
I	1850	382.7 ± 2.3 *0.6*	2150	383.6 ± 1.4 *0.5*	2.82
Te	1850	386 ± 1.8 *0.5*		371.9 ± 2.2 *0.5*	2.4
Ba	1950	403.5 ± 0.9 *0.3*	2150	358.4 ± 1.1 *0.7*	1.1
BaO	1950	391 ± 1.2 *0.76*	2150	424.3 ± 2.1 *0.24*	1.4
Sr	2100	366.1 ± 3.3 *0.1*	2500	349.4 ± 4.7 *0.9*	1.2
La			–	429.3 ± 0.8	2.0
Nd			–	423.5 ± 0.8	2.0
UO_2			–	591.5 ± 1.4	0.4

Please cite this article in press as: J.-P. Hiernaut et al., J. Nucl. Mater. (2007), doi:10.1016/j.jnucmat.2007.03.174

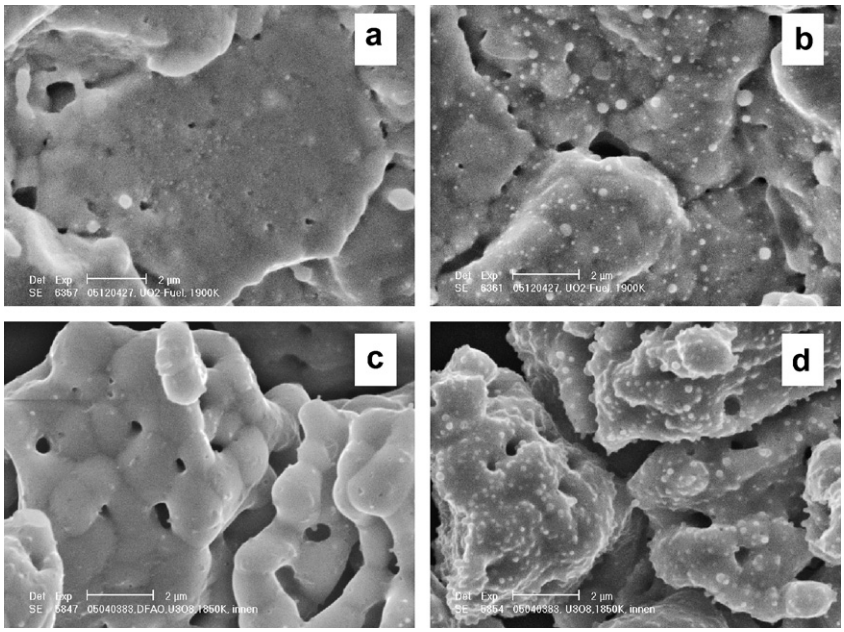

Fig. 5. Secondary electron micrographs showing the irradiated UO_2 samples after annealing at 1900 K: non-oxidised (pictures (a) and (b)) and pre-oxidised (pictures (c) and (d)). Pictures (a) and (c) show external surfaces; pictures (b) and (d) show inner fracture surfaces.

of the pre-oxidised sample. Pictures (a) and (c) show the outer surface of the samples, while pictures (b) and (d) refer to fracture surfaces. The outer surface of UO_2 annealed at 1900 K presented well defined big grains (5–8 μm diameter), with pores present mainly at the grain boundary (picture a). In the oxidised sample, the grains kept a similar size; however, the structure appears much more open and porous (picture c). A large number of metallic precipitates was observed on inner fracture surfaces (pictures b and d), while almost no precipitates were detectable on the outer surfaces (pictures a and c). The metallic precipitates are well visible and are in both cases localised everywhere on the inner surface, not just in voids or pores.

The composition of the metallic precipitates has been determined by EDX. A statistical study on the metals concentration has been done on about 25 precipitates randomly selected on different areas of different parts of both samples. Some results of this analysis are shown in Fig. 6, expressed as average fractional composition normalised to Rh and Pd. A large discrepancy in relative concentration of the five metals has been observed comparing the two samples. The main differences were a large decrease of the Mo concentration from 25–40% in the non-oxidised sample, to 2–7% in the oxidised sample, and a smaller decrease of Tc by a factor 1.6. The concentration of the other metals (Ru, Rh, Pd) remained unchanged for the two samples. No Ru was detected by mass spectrometry. The data in the figure illustrate the main discrepancy between oxidised and non-oxidised UO_2 samples concerning the release behaviour of Mo and Tc species as observed by mass spectrometric measurements during the Knudsen cell annealing test, i.e. the release from the pre-oxidised sample into the vapour phase of redox-sensitive Mo and Tc (mainly as oxides). These fission products were not detected in the vapour phase from the non-oxidised sample,

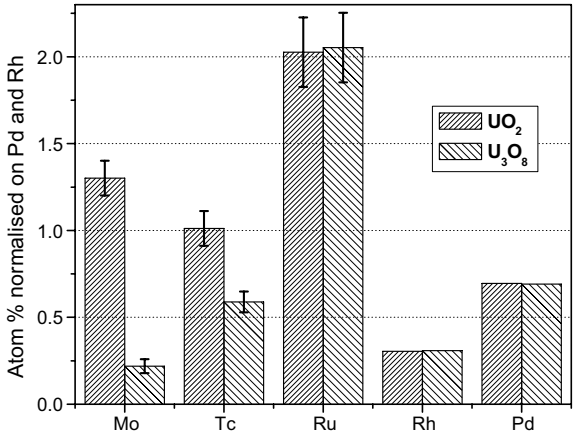

Fig. 6. EDX analysis of the metallic precipitates in irradiated UO_2 and U_3O_{8-x} annealed at 1900 K: average composition hystograms. The values were normalised to Rh + Pd.

Please cite this article in press as: J.-P. Hiernaut et al., J. Nucl. Mater. (2007), doi:10.1016/j.jnucmat.2007.03.174

as expected due to their low vapour pressure in the temperature range considered. These results are consistent with a process consisting of partial depletion of Mo and Tc from the five metal particles and formation of oxide phases of these fission products during the pre-oxidation treatment. Due to their higher volatility, these oxide phases are released during the Knudsen cell annealing in the temperature range up to 1900 K.

5. Discussion and conclusions

The complexity of the system UO_2-fp increases with the $\Delta G(O_2)$. The number and type of phases formed during annealing in presence of a substantial amount of oxygen can be appreciated by analyzing the release behaviour of the fission products and by the post annealing examination of the samples.

The lanthanides that were detected as Ln^+ and LnO^+ in the non-oxidised fuel, are all very soluble as oxide in UO_2. The vapour pressures of the LnO_x species follow Henry's law meaning that their activities are close to their concentrations.

The present results demonstrate that, compared to non-oxides samples, the release of volatile fission products from oxidised material starts at lower temperatures. For example, the maximum release rates for caesium and rubidium are observed at 1250 K in pre-oxidised UO_2 fuel and 1850 K in non-oxidised fuel. This temperature shift of about 600 °C was also found for other volatile fission products (I, Te). The temperature shift for release was significant also for elements like Sr, Ba, Mo, which normally do not belong to the class of volatile fission products. The release rate of Sr and Ba peaked at 1750 K in the case of the pre-oxidised sample, while for non-oxidised fuel the maximum release rate of Sr and Ba occurred at 2500 K and 2100 K, respectively. This must be attributed to the fact that the sample changes its chemical state during the oxidation [3,4], the fission products reacting with each other or with oxygen, forming new compounds and phases that determine a different vaporisation behaviour during the annealing test. Also during the annealing ramp in vacuum in the Knudsen cell the samples transform continuously. The pre-oxidised sample is progressively reduced from U_3O_8 to UO_{2-x}. By the time the sample is reduced to the $UO_{2.00}$ level, corresponding to a temperature of 1900 K, about 100% of the inventory of Sr, Cs, Rb, I and Te has been released, together with 80% Mo and 40 % Tc. Part of these fission products is normally contained in the fuel matrix, with a variable amount that can be considered dissolved in the UO_2 lattice [7]. In order to release the complete inventory of the fission products without vaporizing the whole matrix of the samples different mechanisms have to be considered, involving transport to location from where release occurs at a given temperature (e.g. to grain boundaries), formation of oxidised phases and complexes that can be released as volatiles, precipitation and segregation. In order to interpret the observed behaviour, release curves were analysed with the EFFUS model that permits to define three main stages corresponding to increasing temperature levels: (i) release of fission products that are initially on grain boundaries, (ii) diffusion of dissolved fission products in the bulk followed by eventual precipitation (or phase formation) and release, and (iii) fission products in extended defects (already in other phases) followed by diffusion and vaporisation. The major change of enthalpy between pre-oxidised and non-oxidised samples concerns Cs and Rb in stage II: ΔH_{vap} increases from about 95 kJ mol^{-1}, which is close to the vaporisation enthalpy of metallic Cs (85 kJ mol^{-1}) to 366 kJ mol^{-1} (for Cs) and 360 kJ mol^{-1} (for Rb), which are close to the vaporisation enthalpy of caesium and rubidium oxides [6]. Distinct differences are observed for tellurium, which vaporises for a significant part in stage I in oxidised material, but only in stage II and III in non-oxidised material. This implies that some tellurium is made available for low temperature release during the pre-oxidation treatment. Barium and strontium monoxide are released mainly in stage III in oxidised fuel; however, small amounts of barium and strontium are also released during stage II from non-oxidised fuel. These differences may be due to different location and state of the fission products induced by the pre-oxidation treatment. The vaporisation enthalpies for barium are substantially lower in oxidised fuel. The measured enthalpies in stage III are close to the vaporisation enthalpy of U_3O_8.

Special attention was given to the metallic elements Mo and Tc. At end-of-life most of the Mo and Tc are found in the five metals particles. In contact with O_2 these fission products oxidise depending on $\Delta G(O_2)$. The depletion of the five metals particles in Mo and Tc during the pre-oxidation led to the formation of volatile oxides of these elements that were released during the subsequent Knudsen cell annealing. A higher fraction of Mo inventory was released than that of Tc.

Microscopy examination of both samples after annealing at 1900 K, revealed the presence of

Please cite this article in press as: J.-P. Hiernaut et al., J. Nucl. Mater. (2007), doi:10.1016/j.jnucmat.2007.03.174

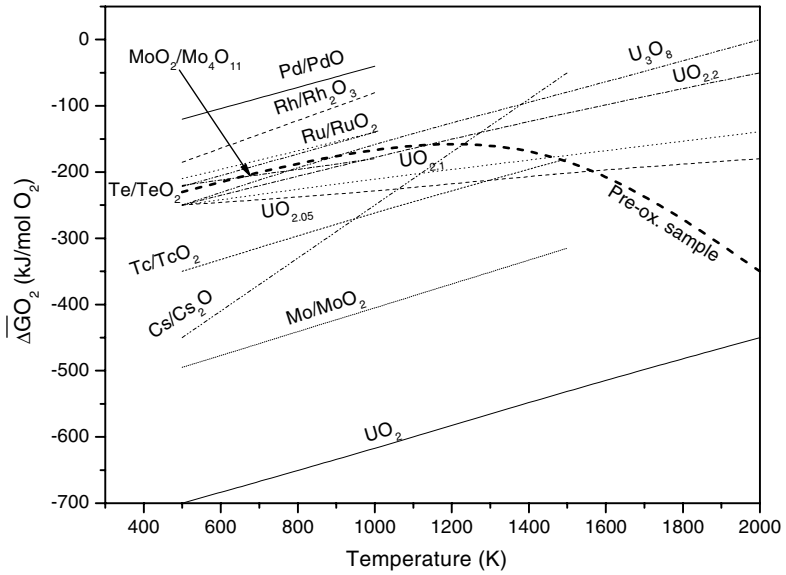

Fig. 7. $\Delta G(O_2)$ vs. temperature of selected volatile fission product species calculated for the samples under Knudsen cell test conditions.

numerous precipitates on the inner fracture surface. EDX confirmed that these were five metals particles. Although a quantitative evaluation of the number and amount of precipitates for the two samples has not been performed, the large number of particles visible on the surface of both samples indicates that this precipitation was temperature driven. The pre-oxidation effect on the five metals particles was limited to the enhanced volatilisation (hence depletion) of the redox-sensitive elements Tc and Mo. It is still not clear why the particles are visible essentially only on inner surfaces.

These observations indicate that the oxidation of the fuel does not lead to a reduction of the release of fission products, but rather to an increase. In the first place, the re-structuring of the fuel caused by oxidation will enhance the segregation of non-soluble fission products from the bulk to grain boundaries and their reaction to form new phases. It was shown previously that oxidised fuel is characterised by fission gas release at lower temperatures [4]. In this work, the early release of tellurium, iodine and caesium observed from the oxidised samples could be due to release from grain boundaries. Direct evidence for the formation CsI as a new phase was found by the observation of the $^{135}Cs^{127}I^{+}$ ion. Our results do not give strong evidence for the formation of Cs_2MoO_4, in absence of the correlation between the Cs and MoO_3 signals. The MoO_3 signal for the oxidised fuel seems to be related to the oxidation/vaporisation of Mo from the metallic inclusions. Technetium is released by the same process.

The release of strontium in monoxide form is essentially complete at 1900 K in the case of the pre-oxidised samples and does not correspond to substantial matrix vaporisation (only about 10% of the fuel matrix vaporises in the temperature range considered). This implies that the pre-oxidation treatment causes a change of state for Sr, which, in turn, results in enhanced volatility during thermal annealing. In the case of barium, the release correlates with the vaporisation of the bulk in both the oxidised and non-oxidised fuel, suggesting that this element remains linked to the fate of the UO_2 lattice [9].

The results obtained are explainable and compatible with the oxygen potentials measured or evaluated in the Knudsen cell and the Gibbs energy of formation of the different fission products oxides reported as an Ellingham diagram in Fig. 7.

Acknowledgements

The authors acknowledge Mr J.-L. Arnould for the sample preparation, MM. F. Capone and J.-Y. Colle for performing Knudsen cell mass spectrometric experiments, and Mr H. Thiele for electron microscopy and EDX analysis. Mr C. Ronchi for developing the EFFUS program.

References

[1] F. Capone, J.P. Hiernaut, M. Martellenghi, C. Ronchi, Nucl. Sci. Eng. 124 (1996) 436.
[2] I. Sato, T. Nakagiri, T. Hirosawa, S. Miyahara, T. Namekawa, J. Nucl. Sci. Technol. 40 (2003) 104.
[3] J.-P. Hiernaut, J.-Y. Colle, R. Pflieger-Cuvellier, J. Jonnet, J. Somers, C. Ronchi, J. Nucl. Mater. 344 (2005) 246.
[4] J.Y. Colle, J.-P. Hiernaut, D. Papaioannou, C. Ronchi, A. Sasahara, J. Nucl. Mater. 348 (2006) 229.
[5] H. Kleykamp, J. Nucl. Mater. 131 (1985) 221.
[6] L.V. Gurvich, V.S. Iorich, D.V. Chekhovskioi, V.S. Yungman, IVTANTHERMO, CRC, Boca Raton, FL, 1993.
[7] H. Kleykamp, J. Nucl. Mater. 206 (1993) 82.
[8] S. Sunder, R. McEachern, J.C. LeBlanc, J. Nucl. Mater. 294 (2001) 59.
[9] H. Kleykamp, Nucl. Technol. 80 (1988) 412.
[10] P. Martin, M. Ripert, G. Carlot, P. Parent, C. Laffon, J. Nucl. Mater. 326 (2004) 132.
[11] I. Sato, H. Furuya, T. Arima, K. Idemitsu, K. Yamamoto, J. Nucl. Mater. 273 (1999) 239.
[12] F.C. Iglesias, B.J. Lewis, P.J. Reid, P. Elder, J. Nucl. Mater. 270 (1999) 21.
[13] J. McFarlane, J.C. LeBlanc, D.G. Owen, AECL 11708 (1996).
[14] S. Sunder, R.F. O'Connor, in: Proceedings of the 8th International Conference on CANDU Fuel, 2003, p. 173.
[15] J. Huang, M. Yamawaki, K. Yamaguchi, M. Yasumoto, H. Sakurai, Y. Suzuki, J. Nucl. Mater. 247 (1997) 17.
[16] J. Huang, M. Yamawaki, K. Yamaguchi, M. Yasumoto, H. Sakurai, Y. Suzuki, J. Nucl. Mater. 248 (1997) 257.
[17] J. Huang, M. Yamawaki, K. Yamaguchi, F. Ono, M. Yasumoto, H. Sakurai, J. Sugimoto, J. Nucl. Mater. 270 (1999) 259.
[18] J. McFarlane, J.C. Wren, R.J. Lemire, Nucl. Technol. 138 (2002) 162.
[19] T.S. Lakshmi Narasimhan, R. Balasubramanian, S. Nalini, M. Sai Baba, J. Nucl. Mater. 247 (1997) 28.
[20] R.R. Hobbins, D.A. Petti, D.L. Hagrman, Nucl. Technol. 101 (1993) 270.
[21] M.F. Osborne, J.L. Collins, R.A. Lorenz, Nucl. Technol. 78 (1987) 157.
[22] B. Andre, G. Ducros, J.P. Lévêque, M.F. Osborne, R.A. Lorenz, D. Maro, Nucl. Technol. 114 (1996) 23.
[23] B.J. Lewis, B.J. Corse, W.T. Thompson, M.H. Kaye, F.C. Iglesias, P. Elder, R. Dickson, Z. Liu, J. Nucl. Mater. 252 (1998) 235.
[24] D.R. Olander, J. Nucl. Mater. 270 (1999) 187.
[25] F. Capone, J.Y. Colle, J.P. Hiernaut, C. Ronchi, J. Phys. Chem. A 103 (1999) 10899.
[26] E.H.P. Cordfunke, R.J.M. Konings, J. Nucl. Mater. 152 (1988) 301.
[27] E.H.P. Cordfunke, R.J.M. Konings, J. Nucl. Mater. 201 (1993) 57.
[28] J.K. Gibson, Radiochim. Acta 60 (1993) 121.
[29] G.J. Darab, P.A. Smith, Chem. Mater. 1996 (1986) 1004.

Please cite this article in press as: J.-P. Hiernaut et al., J. Nucl. Mater. (2007), doi:10.1016/j.jnucmat.2007.03.174